*Nanotechnology Perceptions*
*ISSN 1660-6795*
*www.nano-ntp.com*

# Experimental investigations of Tribological properties of AISID3 Disc and TiN Coated Carbide Pin in LN2 Environment based on Taguchi Technique

**Anurag Sharma**
*Faculty G B Pant DSEU Okhla III Campus*

***Ranganath M Singari***
*Professor, Delhi Technological University*
*ranganathdce@gmail.com*

The effect of the supply of LN2 at the interface of TiN coated carbide pin and AISID3 disc for investigation of tribological properties was carried in the enclosed chamber on a pin on disc tribometer. Experiments were performed to compare tribological properties in dry run condition and the cryogenically cooled environment created by LN2. Design of experiments (DoE) was applied on the basis of L9 [OA] orthogonal array. Speed, load and distance were selected as three sliding parameters. Each was varied to three levels. The results were concluded by using Taguchi (signal-to-noise) ratio and analysis of variance techniques. Both the coefficient of friction and the specific wear rate lowered during cryogenic cooling with LN2 by 20-35% and 21-25% respectively as compared with the dry run condition. SEM microimages of worn-out pins were taken to understand the mechanism of wear. Abrasion and adhesion mechanisms were found during the dry run. SEM micro images of wear tracks showed abrasion and adhesion on low sliding parameters of speed, load and distance. Plastic deformation and fracture were found on high levels ofsliding parameters of speed, load and distance. EDAX of wear tracks of high sliding parameters were taken during dry and cryogenic cooling with LN2. Highpeaks of Fe and O2 were found for both conditions. No traces of nitrogen were found during cryogenic cooling with LN2.

**Keywords:** Cryogenic cooling, liquid nitrogen, Taguchi method, optimization, ANOVA.

## 1. Introduction

Conventional cooling fluids and lubricants are not sufficient to provide a low coefficient of friction and low wear rate for tribo pair like gears-gear, spring-lever etc., operating under extreme conditions of high temperature and high pressure as in spacecraft, rocket propulsion and aviation rafts. The clean and green cooling may be provided by cryogenic fluids such as liquid nitrogen, liquid hydrogen, liquid helium etc. either in closed ducts, closed chamber surrounding tribopairs or at the interface of tribopairs. Liquid nitrogen is the colourless, tasteless, non-toxic and boiling point of -196°C [1-8]. Cryotribometers designed to measure tribological properties of materials by providing similar operating conditions of spacecraft in a dry and cryogenic environment. The Federal Institute of Materials Research and Testing investigated the material behaviour and tribological investigations in specially designed cryotribometers for various ranges of speed, load and sliding distance with $LN_2$ and LHe from 71-4.2°K. It was found that below 4.2°K tribological properties were influenced by low temperature. Friction and wear rate declined for steel-steel and TiN in the absence of oxygen and humidity [9]. Ostrovskayw et al. [10] investigated tribological changes at low temperature in vacuum tribometers from 293-77°K. Cooling was maintained by circulating $LN_2$ in the closed ducts surrounding disc and pin. Friction and wear for a wide range of materials and coatings reduced at low temperature engineering or the field of space vessels and rocket science. Yukikaw et al. [11] investigated tribological properties of graphite and diamond by using pin on disc tribometer in the cryogenic range of 4.2-293°K. Diamond pins were sliding on stainless steel disc coefficient of friction was approximately independent at 4.2°K and 77°K but inclined with velocity 293°K. In diamond/CVD diamond pairs coefficient of friction was maximum at 4.2°K and declined with temperature. Materials sliding against graphite discs showed a peak high for coefficient of friction with temperature 100-200° K due to a decrease in hardness with temperature rise. The effect of coating material at the temperature 4-300°K was analysed. The outcome was that $MoS_2$+Ti coating showed better results than uncoated ones. This created a better practical solution to lubrication during vacuum at a cryogenic temperature [12]. A high cryogenic tribometer was designed by Subramium et al. for evaluation of tribological properties for ball bearings rotating at 36000 rpm under cryogenic environment. This condition was created for space vessels operating under cryogenic temperature. It was found that coefficient of friction was low during cryogenic temperature generated by LHe as compared to $LN_2$ [13].Polymers like polyimide (PI), poly-tetrafluroethylene (PTFE) and polyetheretherketone (PEEK) at cryogenic temperature showed a low coefficient of friction than room temperature. Aromatic thermosetting co-polyster (ATSP) coatings at110MPa showed coefficient friction declined trend with low temperature. It was found that maximum value of coefficient of value was 0.3 at-100°C. After the performance of experiments at low-temperature ATSP and PEEK, coatings showed zero wear. This was shown by using profilometric wear scans. [14-18]. A special sliding block cryotribometer was designed to measure the effect of friction in cryogenic conditions and found that temperature had almost no effect on static and dynamic friction between 4-200°K [19]. Chemically stabled polymer PEEK exhibited improved tribological behaviour in $LH_2$ cryogenic conditions [20]. Tayeb et al. [21] used a direct supply of $LN_2$ at the interface of pin (TI54–titanium alloy) found that wear volume was low during cryogenic condition as compared to room temperature. SUS440C stainless steel balls

were coated with different coatings and tested on ball-on-disk tribometer for1200 seconds at various speed, distance and load constant at 15N in LN2.It was found that coefficient of friction was low at a cryogenic range of temperature maintained by LN2 with a coating of MoS2 [22]. Basu et al. [23] used LN2 supply at the interface of pin and disc in specially designed tribometer. The disc was of high purity copper and steel balls were used for sliding. Low oxygen peaks were found in EDAX of wear disc. This showed oxidation wear as negligible. Delamination and fracture were found on wear tracks of disc [23].

Optimization techniques help in making balanced use of resources. This reduces unnecessary costs involved during machining operations. A planned design of experiments make the process simple and save raw materials, energy and power [24-27]. Researchers conducted several studies to optimize machining responses like surface roughness, tool wear, tool life, residual stresses, etc. under different machining conditions. This may include dry, wet, minimum quantity lubrication, cryogenic cooling with liquid nitrogen or frozen carbondioxide [28-31]. Taguchi method based method on signal-to-noise ratio (S/N) ratio has been used for different types of materials like AISI D3, AISI H13 AISI 4340, EN 19, EN 31, highalloy white cast iron, zirconia toughned aluminia, magnesium, Inconel 718, material created from powder metallurgy, etc., during machining. The machining parameters like (i) speed,
(ii) feed and (iii) depth of cut were optimized for finding the better results for machining responses [32-38]. Some researchers extended the Taguchi signal to noise ratio for finding out wear rate of the fabricated pin through metal composites or cryogenically treated pin on pin-on-disc tribometer [39, 40].

The created $LN_2$ environment does not contain any pollutants and can be readily used for recycling for raw material. The health-related issues regarding respiration, skin infections etc., for the operator may not arise because $LN_2$ is non-toxic. The debris collected could be readily used as scrape free from any harmful chemicals and can save extra cost for handling and decomposing in nature [41-44] AISI D3 is used for making punches, bushes, fabrication of blanking and forming dies, forming tools and wear-resistant moulds. This cold working steel falls under the category of difficult-to-machine material [45].

The review of research papers showed that steel/steel, coated/uncoated alloys, Ti alloy/Ti alloy were used as pin/disc material under dry and cryogenically treated material. Many researchers have suggested that direct supply of LN2 at the interface of cutting tool and workpiece during machining provided improved properties of tribological and machinability characteristics. The novelty of research work is that for enhancing a deeper understanding of frictional and wear behaviour at the interface of cutting tool and workpiece material could only be performed with a dedicated tribometer. This may be due to the fact that no cutting process took place during sliding. This could be simulated the similar tribological and wear behaviour as occurred during machining (i) pressure (ii) force (iii) localized environment at the interface of cutting tool and workpiece. The exhaustive literature review showed that combination of TiN coated carbide (pin) as cutting tool and AISI D3 as (disc) have not been used on pin-on-disc tribometer under dry and cryogenic cooling with $LN_2$ with a specialized fabricated nozzle. This reduced the diameter of pipe from 10mm to 1mm within the length of40mm. This concentrated the flow of $LN_2$ at the interface of pin and disc. Therefore, researchwork focused on the performance of experiments on Taguchi based signal-to-noise ratio L9

[OA] DoE during dry and cryogenic cooling with a direct supply of $LN_2$ at the interface of pin and disc of tribometer in an enclosed chamber. The frictional and wear behaviour were analysed with (ANOVA). Additional results were given regarding the wear behaviour of respective wear tracks of pin during dry and cryogenic sliding.

Nomenclature

µd'= Coefficient of friction during dry sliding

µc'= Coefficient of friction during cryogenic sliding

SwrD'= Specific wear rate during dry sliding

Swr C'= Specific wear rate during cryogenic cooling

S'= Sliding Speed (m/min.)

L'= Load

D'= Sliding distance

Elets= Elements

Wt%= Weight percentage

OA=Orthogonal array

$LN_2$= Liquid nitrogen

DoE= Design of experiments

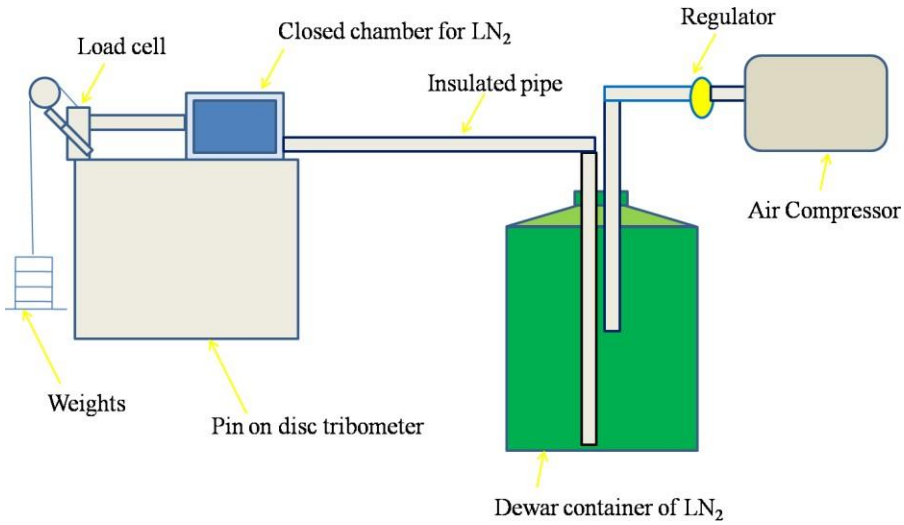


Fig. 1(a) Schematic view of the experimental setup

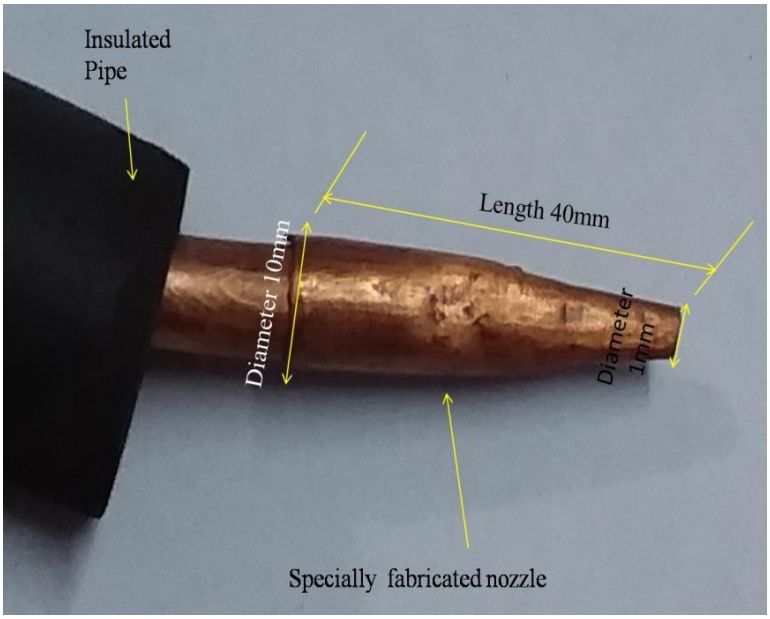


Fig. 1(b) Specially fabricated nozzle

## 2. Experimental materials and methods

2.1 Disc material

Discs were made from AISI D3 steel. The sample of the material was chemically tested before the fabrication of disc.Table1shows the standard elements found in the percentage of weight. The diameter of the disc was 165mm. Thickness was $8^{\pm 0.05}$mm. Four holes of diameter 4mm and length 8 mm were drilled thoroughly at 45°angle to each other. On P.C.D of 155mm.Counterbores at was made for each hole at diameter 8mm and length 4.5mm. The surface of the disc was ground. Surface roughness was measured between 0.12-0.25µm R.M.S. value by Taylor Hobson Surtronic3+ surface roughness tester. 10 readings were taken in the radial direction with an interval of 45°and 10 readings were taken perpendicular to it from the middle stroke of surface roughness tester.

Table1Nominal elements found during chemical analysis test of disc steel material

| Elets | C | Si | Mn | S | P | Cr | Mo | V | W |
|---|---|---|---|---|---|---|---|---|---|
| Wt% | 2.04 | 0.257 | 0.431 | 0.027 | 0.022 | 11.09 | 0.08 | 0.039 | 0.085 |

2.2 Pin material

Pins were made from carbide material in the shape of a cylinder. The diameter was $10^{\pm 0.01}$mm. The height was $35^{+0.00}_{-0.01}$ mm.The pins were coated with TiN in the thickness of 1µm.The sample material of pin was chemically tested for finding out elements. Table 2 shows elements in the percentage of weight.

Table 2 Elements found during chemical analysis test of pin material

| Elets | C | Co | Cr | Fe | W | Ti |
|---|---|---|---|---|---|---|
| Wt% | 7.12 | 12.98 | 0.045 | 0.035 | 30.22 | 49.6 |

Process

A dedicated pin-on-disc tribometer was used for the performance of experiments. The rotating disc could attain a speed in the range of 200-2000rpm. The frictional force could be measured within the maximum value of 200N. The least count was 0.1N. It is shown in Fig.1that amount of weights were placed in the pan of hanger linked to load cell. A dewar container of the capacity of 50kg was used for the storage of $LN_2$. An air compressor was connected to the container. Pressure regulator was fitted in the air supply pipe to containerfor the balanced air supply. The insulated pipe was connected to dewar container and other ends to the closed chamber of pin-on-disc tribometer.

2.3 Design of Experiment

The experiments were performed by generating variations in sliding features to different levels. This was a part of the design of experiments (DoE). The sliding parameters were speed, load, and distance. For full factorial design, a total of $3^3$= 27 experiments were required to be performed. But, according to Taguchi, Design of 9 experiments was needed. This declined more than 50% of experiments. This restricted unnecessary hit and trial of experiments. This saved raw materials for tool and workpiece. This prevented the wastage ofenergy and cutting fluids. Table 3 depicts sliding parameters like sliding speed, load and sliding distance. Each sliding parameter with three levels of variations as Level 1, 2 and 3.This was in respective of incrementing value from lower to next higher. Table 4 depicts theplan of the performance of experiments.Column1 shows experimental trial numbers, column 2, column 3and column 4 show variations in speed, load and distance respectively. Each set of experiment was repeated three times and the average value was calculated to get the final output response. The sets of experiments were performed in dry condition and cryogenic condition.

Table 3 Variation in levels with sliding parameters

| Levels | Sliding parameters | | |
|---|---|---|---|
| | S'(m/min.) | L'(N) | D'(m) |
| Level1 | 27 | 25 | 500 |
| Level2 | 40 | 45 | 1000 |
| Level3 | 80 | 65 | 1500 |

Table 4 Performance of experiment on DoE [OA]L9

| Run | Speed(m/min.) | Load(N) | Distance(m) |
|---|---|---|---|
| 1 | 27 | 25 | 500 |
| 2 | 27 | 45 | 1000 |
| 3 | 27 | 65 | 1500 |
| 4 | 40 | 25 | 1000 |
| 5 | 40 | 45 | 1500 |
| 6 | 40 | 65 | 500 |
| 7 | 80 | 25 | 1500 |
| 8 | 80 | 45 | 500 |
| 9 | 80 | 65 | 1000 |

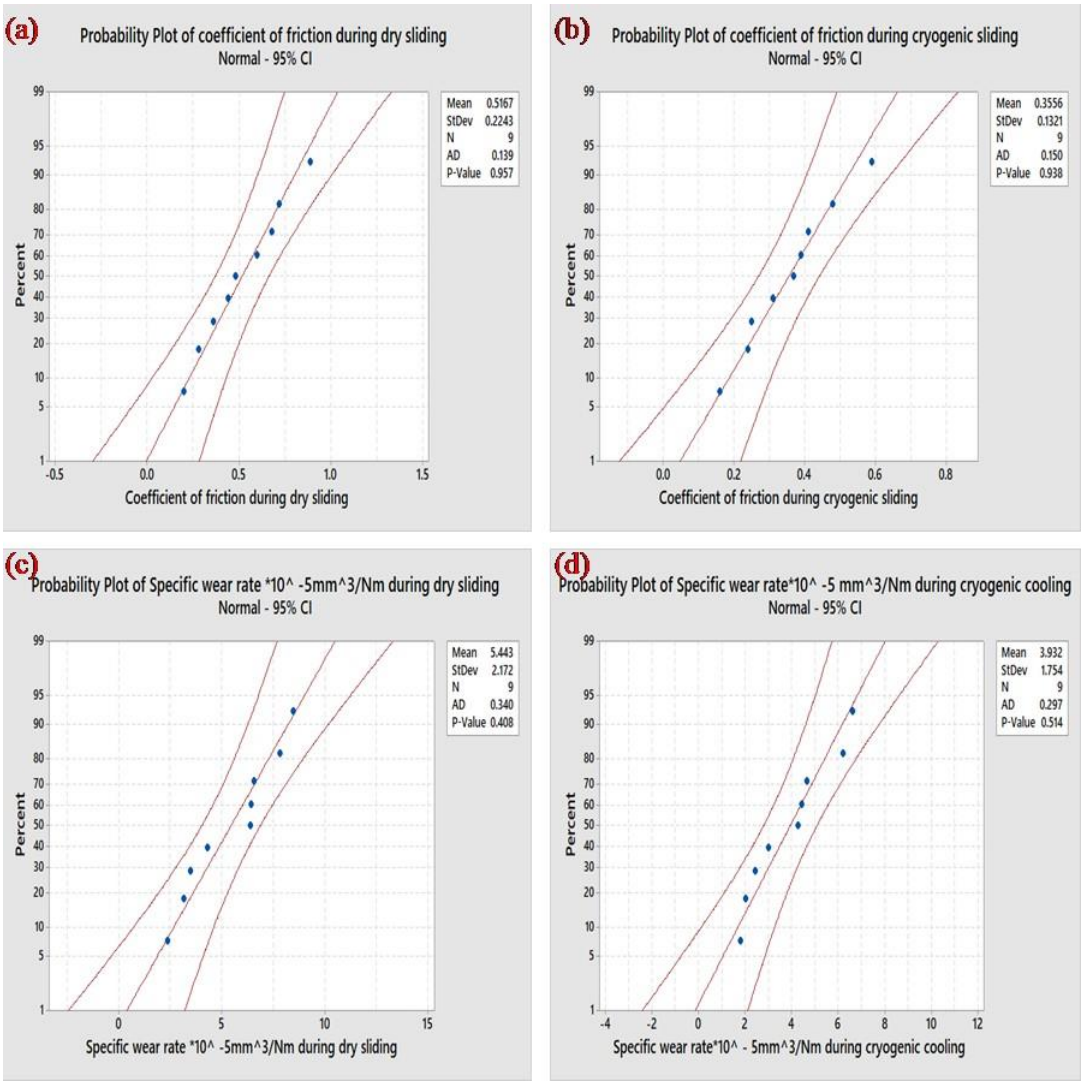


Fig.2 (a) coefficient of friction during dry sliding, (b) coefficient of friction during cryogenic cooling with $LN_2$, (c) specific wear rate during dry sliding and (d) specific wear rate during cryogenic cooling with $LN_2$

## 3. Results and discussion

### 3.1 Analysis by probability plots

Probability plots were made at confidence level of 95% for the result values of experiments. It was depicted in Fig. 2(a) coefficient of friction during dry sliding, (b) coefficient of friction during cryogenic cooling with$LN_2$, (c) specific wear rate during dry sliding and (d) specific wear rate during cryogenic cooling with $LN_2$. It was found from probability plotsthat majority of data points were inclined towards the central line. P-value was greater than

0.01 and AD value was low. This supported that data values were accepted for null hypothesis for normal distribution. This was further used for optimization and analysis of result for making conclusions.

3.2 Taguchi based Optimization

This approach is based on signal- to- noise (S/N) ratios. This is used to measure the extent of achieving the predicted value while considering the noise (uncontrolled factors).The controlled factors were varied with a fixed plan. The results were formed according to the required condition of output. The output may be smaller, medium and larger. Smaller output of result was required in this analysis. The S/N values for coefficient of friction and specific wear rate for dry and cryogenic sliding experiments were calculated for smaller the better characteristics as shown in Eq.1

Smaller is the better characteristic, $\frac{s}{n} = -10\log\frac{1}{n}(x^2)$ (1)

The experiments were performed in dry condition on a pin-on-disc tribometer. The sliding parameters were varied according to L9 [OA] DoE. Analysis of results was done by using Minitab-17software.The output response values (results) are shown in Table 5.The first column shows a sequence of experimental runs. Column second, third and fourth shows sliding parameters like speed, load and distance. Column five and six show output values of coefficient of friction and specific wear rate. Respective S/N value of each experimental run was calculated for output response for coefficient of friction and specific wear rate by using Eq.1. Table 6 shows S/N ratio output response (results) values of coefficient of friction and specific wear rate during cryogenic sliding. The first column shows sequence of experimental runs. Column second, third and fourth shows sliding parameters like speed, load and distance. Column five and six, show output values of coefficient of friction and specific wear rate. Respective S/N value of each experimental run was calculated for output response for coefficient of friction and specific wear rate by using Eq.1

Table 5 Response coefficient of friction (µd'), specific wear rate (SwrD') and S/N values during dry sliding

| Run | during | Parameters | Sliding | | Response | S/N value of response | |
|---|---|---|---|---|---|---|---|
| | Speed(m/min.) | Load(N) | Distance(m) | µc | SwrC | µd | SwrD |
| 1 | 27 | 25 | 500 | 0.20 | 7.81 | 13.9794 | 82.1456 |
| 2 | 27 | 45 | 1000 | 0.28 | 3.16 | 11.0568 | 90.0167 |
| 3 | 27 | 65 | 1500 | 0.44 | 2.37 | 7.1309 | 92.5157 |
| 4 | 40 | 25 | 1000 | 0.36 | 6.57 | 8.8739 | 83.6503 |
| 5 | 40 | 45 | 1500 | 0.48 | 3.49 | 6.3752 | 89.1557 |
| 6 | 40 | 65 | 500 | 0.60 | 6.42 | 4.4370 | 83.8511 |
| 7 | 80 | 25 | 1500 | 0.72 | 6.39 | 2.8534 | 83.8881 |
| 8 | 80 | 45 | 500 | 0.68 | 8.48 | 3.3498 | 81.4298 |
| 9 | 80 | 65 | 1000 | 0.89 | 4.30 | 1.0122 | 87.3270 |

Table 6 Response coefficient of friction (μc'), specific wear rate (SwrC') and S/N values during cryogenic sliding

| Run | during | Parameters | Sliding | | Response | S/N value of response | |
|---|---|---|---|---|---|---|---|
| | Speed(m/min.) | Load(N) | Distance(m) | μc' | SwrC | μc | SwrC' |
| 1 | 27 | 25 | 500 | 0.16 | 6.21 | 15.9176 | 84.1331 |
| 2 | 27 | 45 | 1000 | 0.25 | 2.42 | 12.0412 | 92.3366 |
| 3 | 27 | 65 | 1500 | 0.37 | 1.80 | 8.6360 | 94.9032 |
| 4 | 40 | 25 | 1000 | 0.24 | 4.26 | 12.3958 | 87.4102 |
| 5 | 40 | 45 | 1500 | 0.31 | 2.01 | 10.1728 | 93.9560 |
| 6 | 40 | 65 | 500 | 0.39 | 4.64 | 8.1787 | 86.6633 |
| 7 | 80 | 25 | 1500 | 0.41 | 4.44 | 7.7443 | 87.0555 |
| 8 | 80 | 45 | 500 | 0.48 | 6.61 | 6.3752 | 83.5981 |
| 9 | 80 | 65 | 1000 | 0.59 | 3.00 | 4.5830 | 90.4448 |

Table7 shows data for coefficient of friction and specific wear rate during dry and cryogenic sliding. The sliding parameters are control factors. Delta shows the difference between the maximum and minimum value of the mean S/N ratio for particular control factor. The larger value of delta shows more impacting factor. Rank is given from 1-3.The importance of preference is given from corresponding decreasing order. Rank1 is of higher importance and further decreases to lower. It is shown in Table7, that delta value was higher and rank first

was given to sliding speed for coefficient of friction during dry and cryogenic sliding. Sliding speed was more significant. Delta value was higher and rank first given to distance for specific wear rate during dry and cryogenic sliding. Distance was more significant.

Table 7 Response table for S/N ratio analysis for coefficient of friction (μd', μc') and specific wear rate (SwrD', SwrC') during dry and cryogenic sliding

| Response | Level | S'(m/min.) | L'(N) | D'(m) |
|---|---|---|---|---|
| μd | 1 | 10.722 | 8.569 | 7.255 |
| | 2 | 6.562 | 6.927 | 6.981 |
| | 3 | 2.405 | 4.193 | 5.453 |
| | Delta | 8.317 | 4.376 | 1.802 |
| | Rank | 1 | 2 | 3 |
| μc | 1 | 12.198 | 12.019 | 10.157 |
| | 2 | 10.249 | 9.530 | 9.673 |
| | 3 | 6.234 | 7.133 | 8.851 |
| | Delta | 5.964 | 4.887 | 1.306 |
| | Rank | 1 | 2 | 3 |
| SwrD | 1 | 88.23 | 83.23 | 82.48 |
| | 2 | 85.55 | 86.87 | 87.00 |
| | 3 | 84.21 | 87.90 | 88.52 |
| | Delta | 4.01 | 4.67 | 6.04 |
| | Rank | 3 | 2 | 1 |
| SwrC' | 1 | 90.46 | 86.20 | 84.80 |
| | 2 | 89.34 | 89.96 | 90.06 |
| | 3 | 87.03 | 90.67 | 91.97 |
| | Delta | 3.42 | 4.47 | 7.17 |
| | Rank | 3 | 2 | 1 |

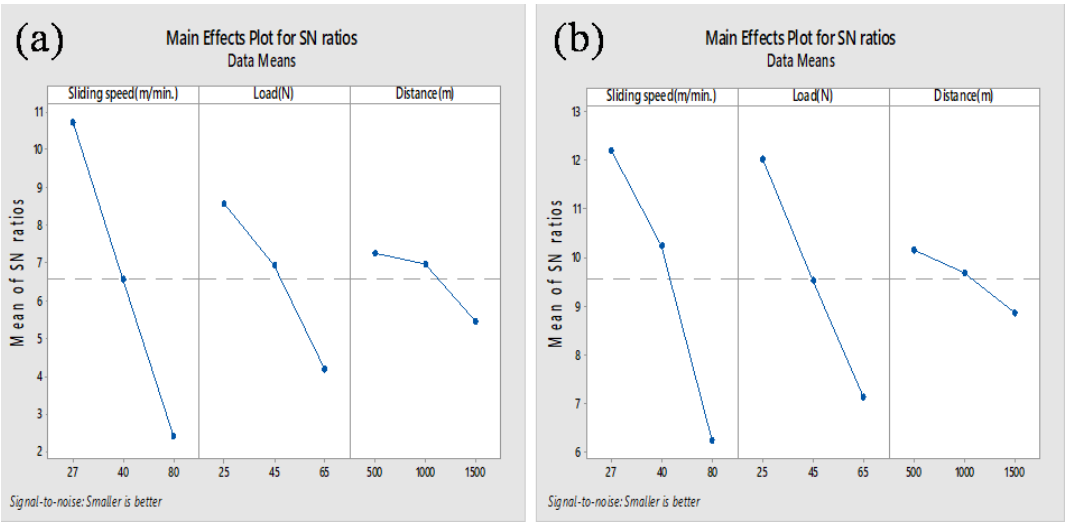


Fig.3 (a) Variation of mean S/N ratio coefficient of friction during dry sliding (b) cryogenic sliding with different factors

Fig.3 (a) shows a variation of means S/N ratio coefficient of friction during dry sliding (b) cryogenic sliding. On incrementing speed, load and distance S/N value of coefficient of friction incremented during dry sliding and cryogenic sliding. The optimized levels of sliding parameters for minimum coefficient friction for dry and cryogenic sliding were at (S'=27m/min.), (L'=25N) and (D'=500m) for dry and cryogenic sliding. Optimized values of coefficient of friction were 0.21 and 0.17 during dry sliding and cryogenic sliding as calculated from Eqs. (2) and (3).

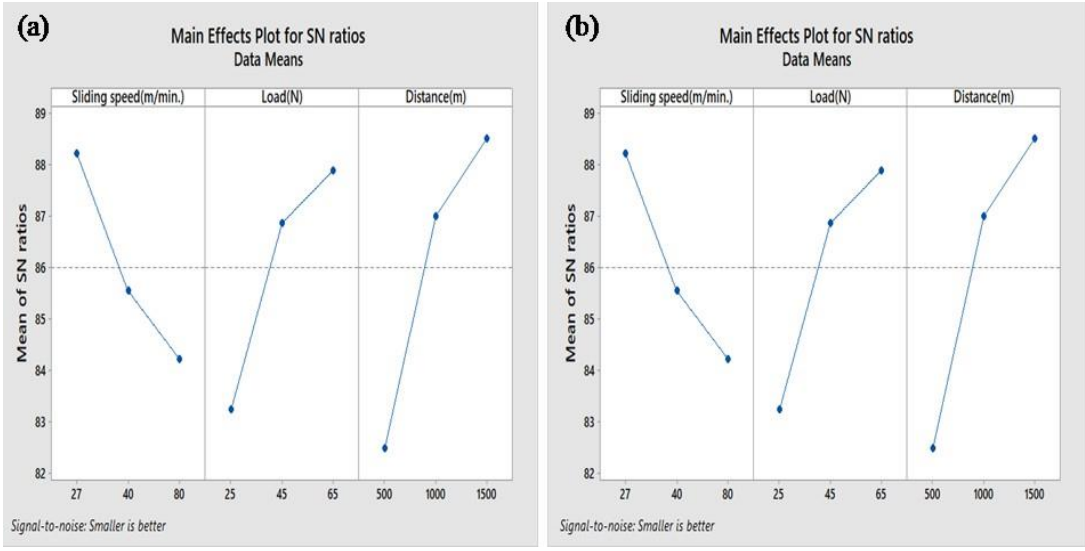


Fig.4 (a) Variation of mean S/N ratio specific wear rate during dry (b) cryogenic sliding with different factors

It is depicted in Fig.4(a) Variation of mean S/N ratio specific wear rate during dry sliding (b) cryogenic sliding with different factors like speed, load and distance S/N value of specific wear rate declined with incrementing sliding speed but incremented with increasing load and distance during dry and cryogenic sliding. The optimized level of sliding parameters for minimum specific wear rate was at (S'=27m/min.), (L'=65N) & (D'=1500m) for dry sliding and cryogenic sliding. Optimized value of specific wear rate was found $2.3297 \times 10^{-5}$ $mm^3$/Nm and $1.7358 \times 10^{-5} mm^3$/Nm during dry and cryogenic sliding respectively as calculated from Eqs. (2) & (3).

$$\lambda p = \overline{\lambda p} + (\overline{So} - \overline{\lambda p}) + (\overline{Lo} - \overline{\lambda p}) + (\overline{Do} - \overline{\lambda p}) \quad (2)$$

$$Bp = 10^{-\lambda p/20} \quad (3)$$

3.3 Analysis of Variance (ANOVA) and the impact of sliding parameters on responses

ANOVA was used for finding out the influence of sliding parameters on particular response value in different environment sliding conditions Table 8 shows first column for the response as coefficient of friction and specific wear rate during dry and cryogenic conditions. Second column shows the source like speed, load, distance, error and total. Third, fourth, fifth and

Sixth columns show DF as a degree of freedom, adjusted sum of squares, adjusted mean squares and F-value respectively. The higher F-value shows the greater influence of sliding parameter for a particular response. Seventh column shows a significant level of 5% at 95% confidence interval. Eighth column shows the percentage of contribution of sliding parameter. From Table 8, coefficient of friction during dry sliding had high F-value forspeed, p-value was significant for speed. The highest effect of percentage of contribution was for speed at 73.95%, next followed by load at 20.90% and finally followed by distance at 4.03%.Coefficient of friction during cryogenic sliding had high F-value for speed, p-value was significant for speed. The highest effect of percentage of contribution was for speed at 57.82%, next followed by load at 37.33% and finally followed by load at 2.73%. Specificwear rate during dry sliding had highest F-value for distance, p-value was significantfor speed, load and distance. The highest effect of contribution was for distance at 49.15%, next followed by load at 29.93% and finally followed by speed at 20.74%. Specific wear rateduring cryogenic sliding had highest F-value for distance, p-value was significant for load and distance. The highest effect of contribution was for distance at 60.35%, next followed byload at 25.25% and finally followed by speed at 13.34%

Table 8 (ANOVA) Analysis of variance for means of coefficient of friction (μd', μc') and specific wear rate (SwrD', SwrC') during dry and cryogenic sliding

| Response | Source | DF | AdjSS | AdjMS | F-Value | p- Value | % |
|---|---|---|---|---|---|---|---|
| μd | S'(m/min.) | 2 | 103.766 | 51.8828 | 65.85 | 0.015 | 73.95 |
| | L'(N) | 2 | 29.314 | 14.6572 | 18.60 | 0.051 | 20.90 |
| | D'(m) | 2 | 5.658 | 2.8288 | 3.59 | 0.218 | 4.03 |
| | Error | 20 | 1.576 | 0.7879 | - | - | 1.12 |
| | Total | 26 | 140.313 | - | - | - | 100 |
| μc | S'(m/min.) | 2 | 55.489 | 27.745 | 27.26 | 0.035 | 57.82 |
| | L'(N) | 2 | 35.824 | 17.912 | 17.60 | 0.054 | 37.33 |
| | D'(m) | 2 | 2.616 | 1.308 | 1.29 | 0.438 | 2.73 |
| | Error | 20 | 2.035 | 1.018 | - | - | 2.12 |
| | Total | 26 | 95.965 | - | - | - | 100 |

| | | | | | | | |
|---|---|---|---|---|---|---|---|
| SwrD | S'(m/min.) | 2 | 25.025 | 12.5127 | 121.55 | 0.008 | 20.74 |
| | L'(N) | 2 | 36.115 | 18.0576 | 175.41 | 0.006 | 29.93 |
| | D'(m) | 2 | 59.302 | 29.6512 | 288.03 | 0.000 | 49.15 |
| | Error | 20 | 0.206 | 0.1029 | - | - | 0.18 |
| | Total | 26 | 120.649 | - | - | - | 100 |
| SwrC | S'(m/min.) | 2 | 18.310 | 9.1548 | 12.64 | 0.073 | 13.34 |
| | L'(N) | 2 | 34.656 | 17.3279 | 23.92 | 0.040 | 25.25 |
| | D'(m) | 2 | 82.825 | 41.4124 | 57.16 | 0.017 | 60.35 |
| | Error | 20 | 1.449 | 0.7245 | - | - | 1.06 |
| | Total | 26 | 137.239 | - | - | - | 100 |

### 3.4 Confirmatory tests at optimized levels

Table 9 shows the first column for the category of response as coefficient of friction and specific wear rate. Second column shows different values of sliding parameters as speed, load and distance at the optimized level. Third column shows predicted value. Fourth columnshows experimental values of results obtained and fifth column shows the percentage of error.

The experiments were performed again at the optimized level for coefficient of friction during dry and cryogenic sliding at speed = 27 (Level=1), load = 25 (Level=1) and distance =500 (Level=1).Other sets of experiment were performed at an optimized level for specific wear rate during dry and cryogenic sliding at speed =27 (Level=1), load = 65(Level=3) and distance = 1500 (Level=3). Each experiment was repeated three times and the average was calculated for the final value. The values of optimized sliding parameters for each response in the distinguished sliding environment of dry and cryogenic with predicted and experimental values are shown in Table 9. It was found that predicted and experimental values were very close to each other

Table 9.Confirmatory table at optimized levels of sliding parameters

| Response | Sliding parameters at optimum level | | | Predicted value of result | Experimental value of | % of Error |
|---|---|---|---|---|---|---|
| - | Speed | Load | Distance(m) | - | - | - |
| μd | 27 | 25 | 500 | 0.21 | 0.21 | 0 |
| μc | 27 | 25 | 500 | 0.17 | 0.16 | 5.88 |
| SwrD | 27 | 65 | 1500 | $2.3297 \times 10^{-5}$ | $2.3295 \times 10^{-5}$ | 0.008 |
| SwrC | 27 | 65 | 1500 | $1.7358 \times 10^{-5}$ | $1.7356 \times 10^{-5}$ | 0.012 |

### 3.5 Evaluation of coefficient of friction

Sophisticated and fine sensors of pin-on-disc tribometer directly measured the friction force. The measurement of friction force was from the start to the end of the experimental run Coefficient of friction was calculated for each experiment using Eq,(4)

$$\mu = \frac{\text{Friction force}}{\text{Load}} \qquad (4)$$

Bar and line graphs were formed by using Origin2018 software.Fig.5 shows a bar graph between coefficient of friction and experimental run. It is depicted that value of coefficient of friction during cryogenic sliding was lower than dry sliding from experimental run 1-9. At slow sliding parameters at experimental run1(S'=27m/min, L'=25NandD'=500m) coefficient of friction was low for dry and cryogenic sliding and at high sliding parameters at experimental run 9 (S'=80m/min, L'=65N and D'=1000m) coefficient of friction was higher, but in all the stages of experiment t coefficient of friction during cryogenic sliding was

lower. This may be due to high efficiency of $LN_2$ in removing heat from the interface of pin and disc. $LN_2$ formed a fluid/gas layer and produced lubrication between pin disc byabsorbing heat and evaporating speedily.

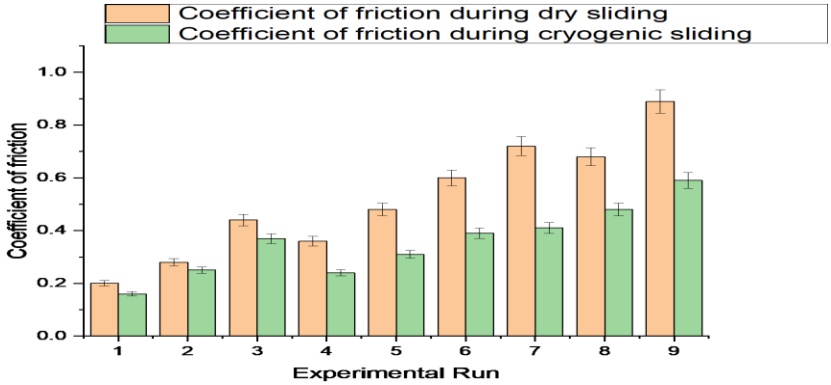


Fig. 5 Values of coefficient of friction during dry and cryogenic sliding as per $L_9$ [OA]

Main effects plots for coefficient of friction with varying speed, load and distance were made as shown in Fig. 6(a), (b) and (c). Fig.6 (a) shows, on incrementing speed from 27-80m/min., coefficient of friction was increasing in both dry as well as cryogenic condition. This may be due to high heat generation and accumulation at the interface of pin and disc but according to the property of $LN_2$in absorbing heat and cooling at a fast rate during cryogenic sliding coefficient of friction was lower than dry sliding. Fig. 6 (b) shows, on incrementing load from 25-65N coefficient of friction was increasing in both dry and cryogenic condition. This may be due to increased pressure generated between pin and disc. This may also increase more heat creation but during cryogenic sliding coefficient of friction was lower than dry sliding. Fig. 6(c) shows on incrementing distance from 500-1500m coefficient of frictionwas more in both dry and cryogenic sliding. This may due to increasing distance also increased contact time between pin and disc. This may lead to heat generation and accumulation for a longer time. This may deteriorate the pin and disc surface. During dry sliding due to high heat, generation increased the coefficient of friction reached to higher values of sliding distance from 500-1000m but due to fast heat removing capacity of $LN_2$and providing fluid lubrication coefficient of friction increased at small intervals to low values. This created a large variation between dry and cryogenic sliding.

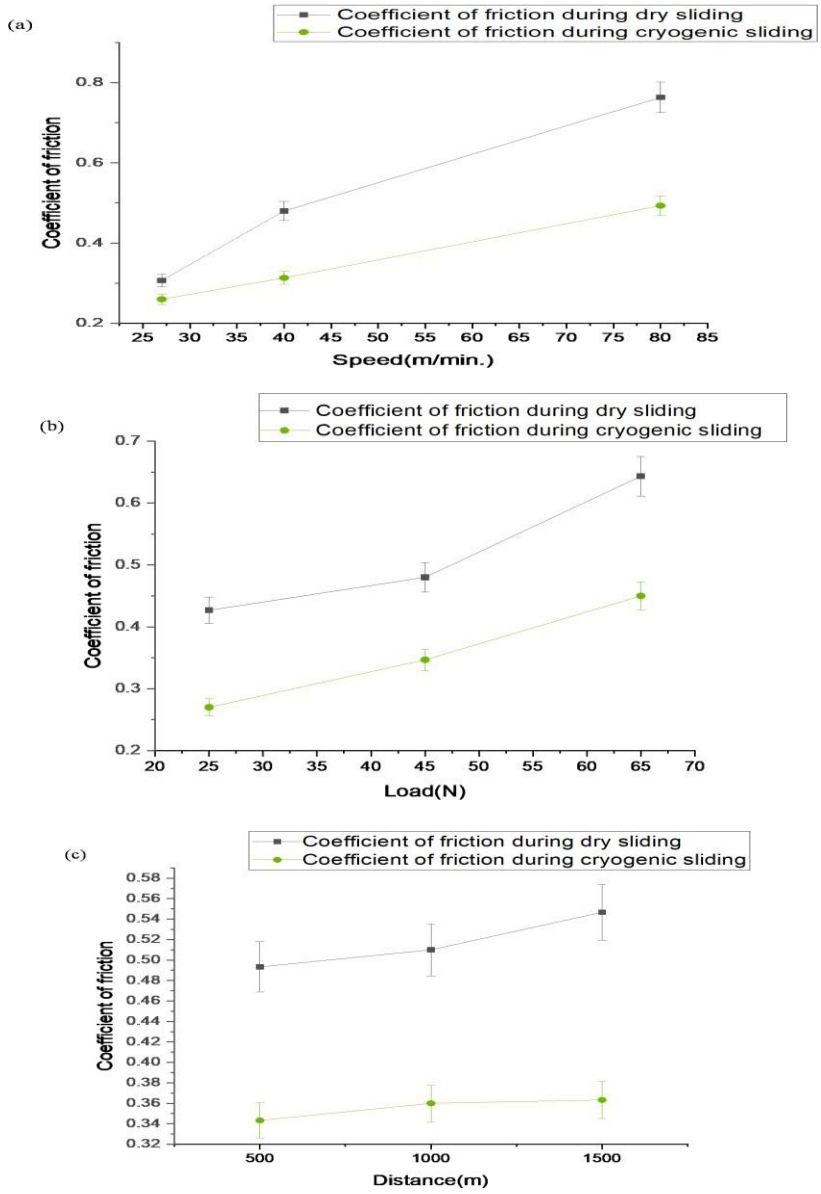


Fig. 6 Main effects plot for coefficient of friction with varying (a) speed, (b) load and (c) distance

## 3.6 Evaluation of specific wear rate

Every pin was weighed before the start and after the completion of each experimental run on the digital electronic balance. The least count was 0.0001g. This was repeated five times and average value was calculated for the final value of the weight. The difference of weight was converted into volume loss(Δ) by using Eq.5 and Specific wear rate was calculated by

$$\Delta V = \frac{Wi - Wf}{\rho} X1000 \qquad (5)$$

Where,

Wi = weight of the pin before the start of the experimental run

Wf = weight of the pin after the end of the experimental run

ρ = Density of pin material

$$Swr = \frac{\Delta V}{F^F \times S^F} \qquad (6)$$

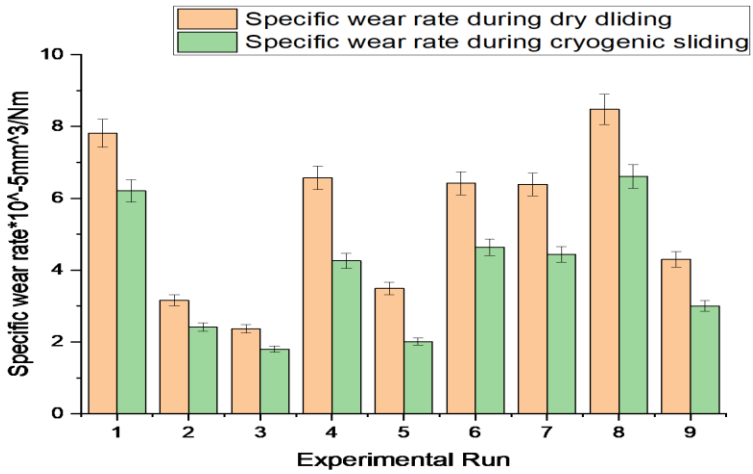


Fig.7 Values of specific wear rate during dry and cryogenic sliding as per $L_9$ [OA]

Fig.7 shows bar graph between specific wear rate and experimental run. It is depicted that value of specific rate during cryogenic sliding was lower than dry sliding from experimental run1-9.At slow sliding parameters at experimental run3 (S'=27m/min, L'=65NandD'=1000m) specific wear rate was low for dry and cryogenic sliding and at high sliding parameters at experimental run 8 (S'=80m/min, L'=45N and D'=500m) specific wear rate was high, but in all the stages of experiment, specific wear rate during cryogenic sliding was lower. This may be due to the pressurized supply of $LN_2$ at the interface of pin and disc. The debris generated was taken away from the contact surface. This made the surface neat and clean.

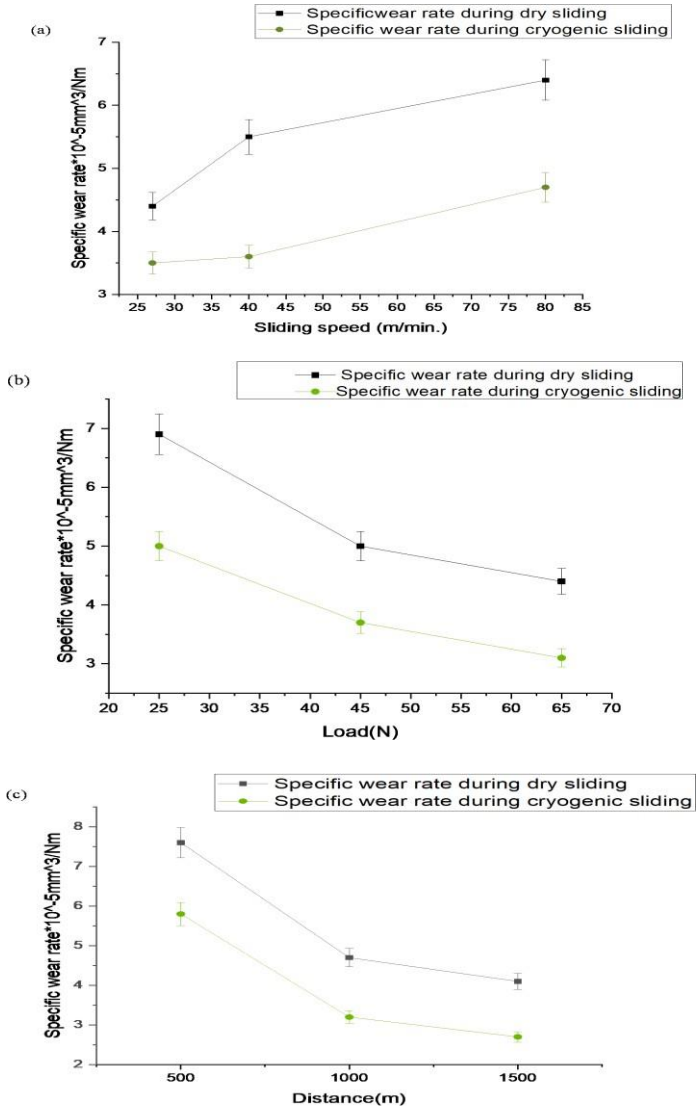


Fig.8 Main effects plot for specific wear rate with varying (a) speed, (b) load and (c) distance

Main effects plots specific wear with varying speed, load and distance were made as shown in Fig.8 (a), (b) and(c) Fig.7(a) shows, on incrementing speed from 27-80m/min., specific wear rate was increasing in both dry as well as cryogenic condition. The value of specific wear rate was found to be lower. This may be due to better heat removing property of LN2. Fig. 8(b) shows, on incrementing load from 25-65N specific wear rate was declining in both dry and cryogenic condition. The value of specific wear rate was lower for the cryogenic condition.Fig.8(c)shows on incrementing sliding distance from 500-1500m specific wear rate was declining in both dry and cryogenic sliding. The value of specific wear rate was lower for cryogenic condition. This may be due better cooling created.

3.7 Pin wear mechanism.

Fig. 9(a) depicts SEM micro image of the worn out pin at low sliding parameters S'=27m/min., L'=25N and D'=500m during dry sliding (without any lubricant) after the end of experimentalrun'1'. It was found that wear scar from the middle portion to the outer edge. On increasing the magnifying scale. Edges fracture was noticed with parallel inclined grooved lines. This showed the abrasion mechanism wear. This may be due the debris particles got accumulated between pin and disc surface. Fig. 10 (a) depicts SEM micro image at higher sliding parameters S'=80m, L'=65Nand D'=1000m. The small depressions were seen at the middle portion of the pin. On increasing magnifying scale wider edge broken was viewed. This may be due to the increase in pressure applied on pin and increment in real contact area. Fig. 9 (a) depicts SEM micro image of worn out pin during cryogenic cooling with $LN_2$ supply at the interface of pin and disc at low sliding parameter atS' =27m/min., L'=25N and D'=500m. It was found that pin surface found smooth and clean Negligible minor edge fracture was found on the magnifying scale. Fig. 10(b) depicts SEM image at higher sliding parameters at S'=80m, L'= 65N and D'=1000m. The surface was smooth without any cavities. Negligible minor edge fracture was found on the magnifying scale. This may be due to high efficiency of $LN_2$ in removing heat from the interface of pin and disc. Low friction reduced the deterioration of the surface of the pin.

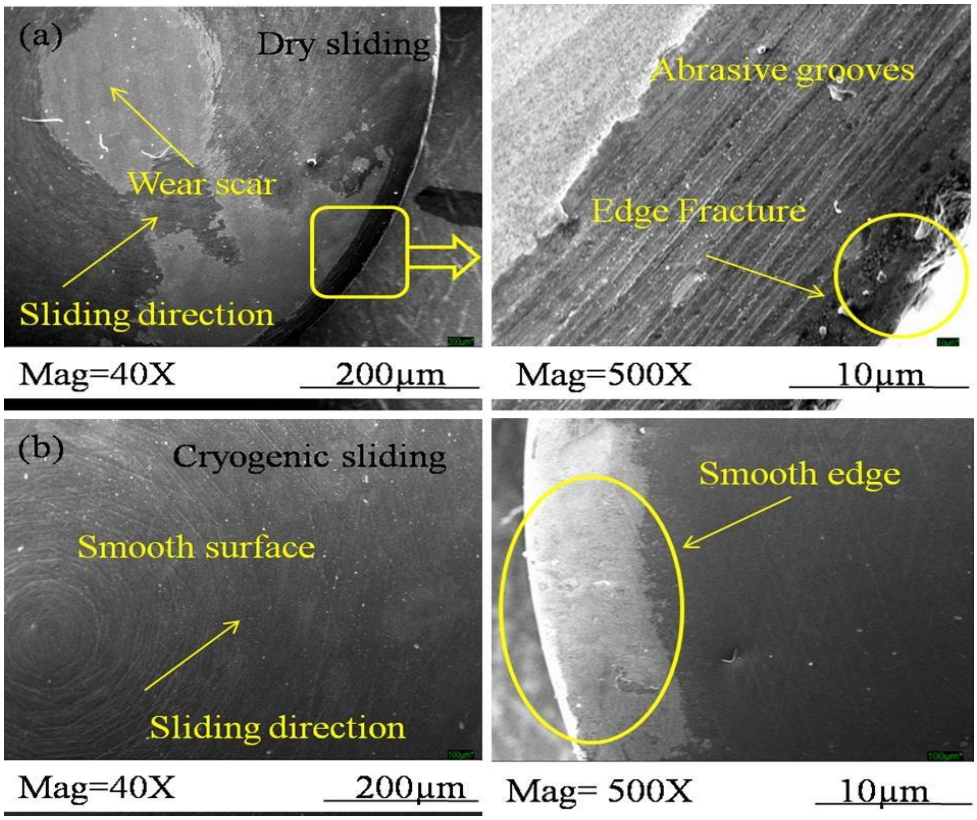


Fig.9 SEM image of worn out pin at sliding parameters S'=27/min., L'=25N and D'=500m

(a) dry & (b) cryogenic sliding

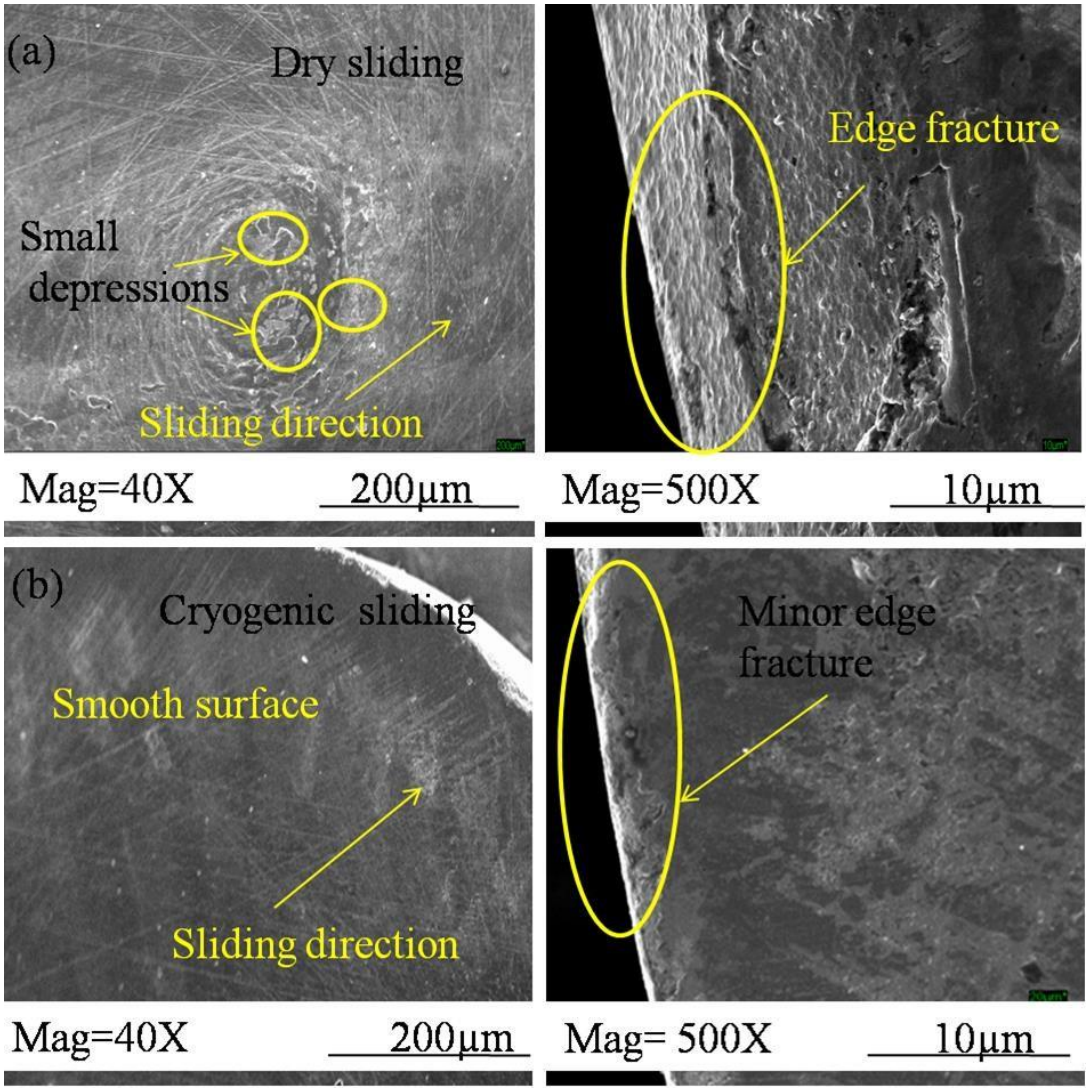


Fig.10 SEM image of worn out pin at sliding parameters S'=80/min., L'=65NandD'=1000m (a) dry & (b) cryogenic sliding

3.8 Wear mechanism of wear tracks of disc:

Fig. 11 (a) depicts SEM micro image of wear track at low sliding parameters S'=27m/min., L'=25N and D'= 500m during dry sliding (without any lubricant) after the end of experimental run‘1’. Grooves and delamination were observed. On magnifying scale wear debris was observed on wear track with ploughs. This showed abrasion wear mechanism. Debris got accumulated and generated grooves. The friction increased. This might increment heat generation and a certain weaker portion of wear track got removed causing cavities and fracture. Fig. 12(a) depicts SEM micro image of wear track at higher sliding parameters S'=80m/min., L'=65N and D'=1000 m during dry sliding (without any lubricant) after the end of experimental run‘9.’ The pressure on pin increased. This may increase the real contact

area between pin and disc. The grooves became deeper. High heat generation and accumulation gave rise to plastic deformation and fracture. The abrasion, adhesion and oxidation wear mechanism were present. Fig. 11(b) depicts SEM micro image of the wear track of disc at low sliding parameters S'=27m/mi., L'=25N and D'=500m during cryogenic sliding with $LN_2$ after the end of experimental run'1'. The surface of wear track was neat, clean and smooth. On magnifying SEM image, the surface of wear track was found to be smooth. Fig. 12(b) depicts SEM micro image of wear track at high level sliding parameters S'=80m/min., L'=65N and D'=1000m during cryogenic sliding with $LN_2$ after the end of experimental run '9'. This showed negligible shallow and small cavities. On the magnifying scale some shallow grooves. This may due to high pressure on pin and disc. This increased the real contact area between pin and disc. But, due to the property and efficiency of $LN_2$ in removing heat quickly. The temperature reduced to multiple times. The surface was smooth and clean as compared to the dry condition due to high-pressure supply of $LN_2$ at the interface of pin and disc. This washed away debris away from the wear track.

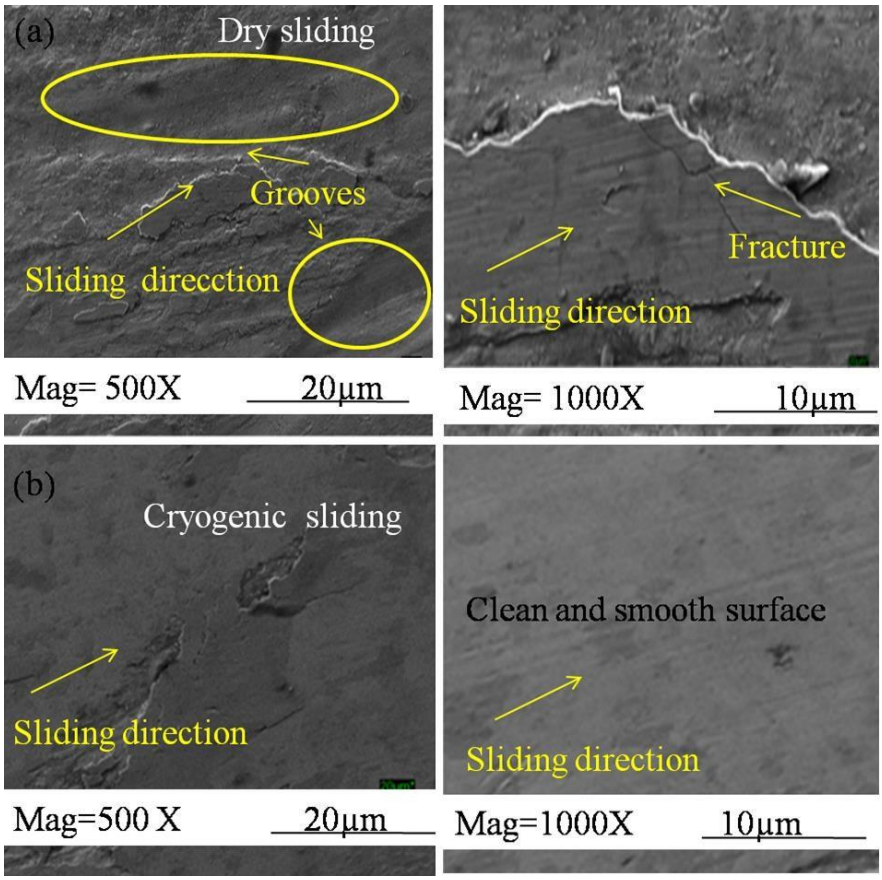


Fig.11 SEM image of wear track formed on the disc at S'=27/min., L'=25N and D'=500m (a) dry & (b) cryogenic sliding

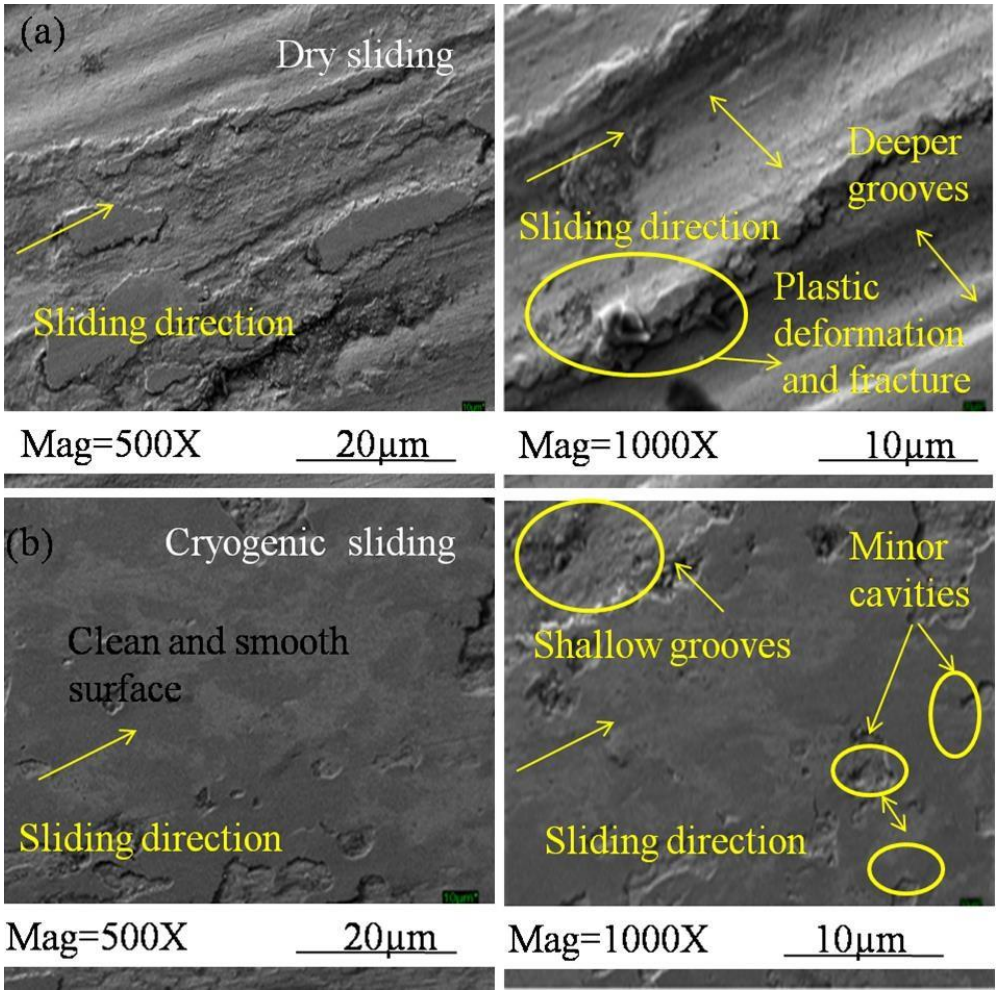


Fig.11SEM image of wear track formed on the disc S'=80/min., L'=65N and D'= 1000m (a) dry & (b) cryogenic sliding

3.8 SEM micro image with EDS spectrum of wear track

SEM micro image with EDS spectrum of wear track during dry sliding is shown as Fig. 13(a) and (b) at experimental run 9ʾ at sliding parameters of S'=80 m/min., L'=65N and D'=1000m. The surface was found with delamination due to the formation of cavities. High peaks of Fe and O2 were observed. Fig. 14(a)and (b) depict SEM micro image with EDS of wear track during cryogenic sliding with $LN_2$ direct supply at the interface of pin and disc with sliding parameters of experimental run 9ʾ at sliding parameters of S'=80 m/min., L'=65N and D'=1000m. The surface found to be smooth and clean with respect to dry slidingcondition. The high pressure jet of $LN_2$ washed away debris from the wear track. The coolingefficiency of $LN_2$ kept away the heat accumulation at the contact site. This saved the surface from deterioration High peaks of Fe, $O_2$ were observed on wear track but no traces of nitrogen was found. This showed that $LN_2$ non-reactive with the material.

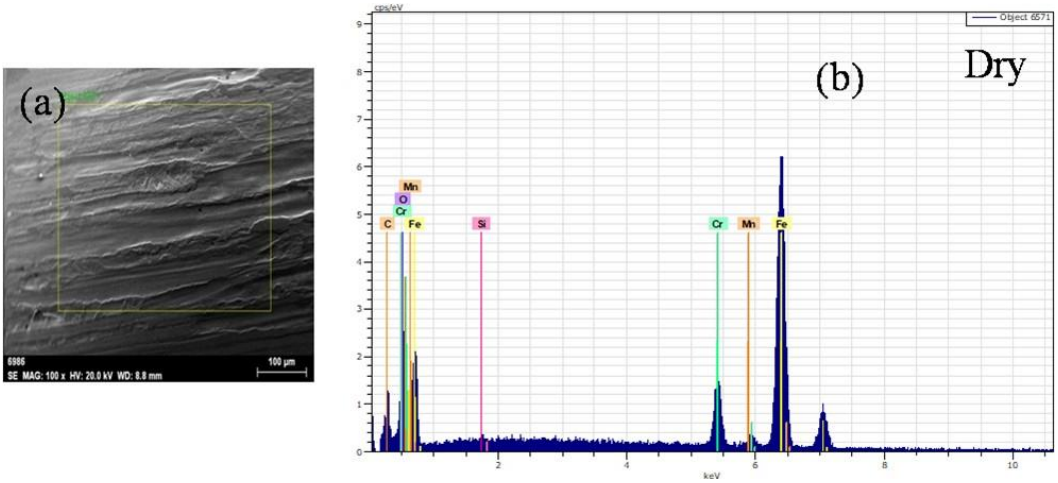


Fig. 13(a) SEM image, (b) EDS at S'=80/min., L'=65N and D'= 1000m during dry sliding

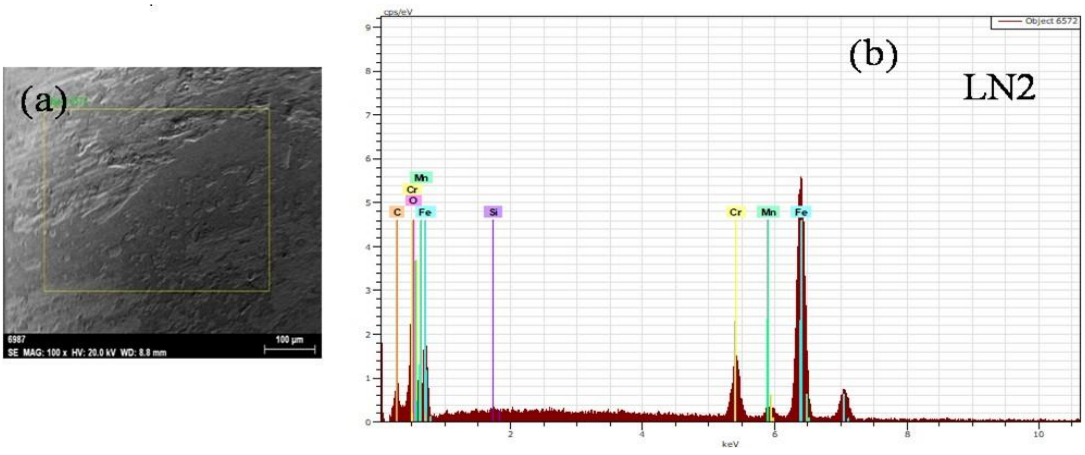


Fig. 14(a) SEM image, (b) EDS at S'=80/min., L'=65N and D'= 1000m cryogenic sliding with $LN_2$

## 4. Conclusions:

Sliding experiments were performed on pin-on-disc tribometer with AISI D3 as disc material and TiN coated as titanium carbide pin material on various relative speed, normal load and sliding distance. The experiments were carried according to L9 DoE in dryroom condition and cryogenic cooling created $LN_2$ environment. The major conclusionshave been summarized as follows:

1 The coefficient of friction lowered by 20-35% during cryogenic sliding with $LN_2$ as compared with the dry run (without any lubricant). In such condition, liquid nitrogen helped in removing heat generated at the interface of pin and disc.

2 The specific wear rate declined by 21-25% during cryogenic sliding with $LN_2$ as compared with the dry run (without any lubricant). Liquid nitrogen absorbed the heat at a very fast rate and formed a fluid/gas film at the contacting surface. This helped in low wear during cryogenic cooling with $LN_2$.

3 SEM micro images analysed for worn out TiN coated pins showed abrasion and adhesion wear mechanisms. Edge fracture was found at the corners during dry sliding. Worn out pin during cryogenic cooling with $LN_2$ showed clean and smooth surface.

4 SEM micro images were analysed for wear tracks of AISID3 disc showed abrasion and adhesion wear mechanism were present at low sliding parameters of speed, load and distance. Plastic deformation and fracture at high sliding parameters. Wear tracks during cryogenic cooling with $LN_2$ clean and smooth surface. This may be due to fast heat removing capacity of liquid nitrogen.

5 The minimum coefficient of friction was found at sliding parameters (S', Level=1), (L', Level=1) and (D', Level=1) during dry and cryogenic sliding. These were the optimized level for coefficient of friction.

6 The minimum specific wear rate was found at sliding parameters (S', level=1) and (L', Level=3) and (D', level=3) during dry and cryogenic sliding. These were the optimized level for specific wear rate.

Acknowledgements: Authors are highly thankful for the help given from laboratories and workshop of Delhi Technological University and Indian Institute of Technology, Delhi,India.

**References**

1. Byrene, G.; Scholta, E.: Environmentally clean machining processes-a strategic approach.CIRP Annals – Manufacturing Technology 42(1), 471-474 (1993)
2. Hong, S. Y.; Zaho,: Thermal aspects, material consideration and cooling strategies in cryogenic machining. Clean Production Processes 1107-116 (1999)
3. Wang, Z. Y.; Rajurkar, K. P.: Cryogenic machining of hard-to-cut materials. Wear 239, 168-175(2000)
4. Hong, S. Y.; Broomer, M.: Economical and ecological cryogenic machining of AISI 304 austenitic stainless steel. Clean Technology Environment Policy 2(3), 157-166 (2010)
5. Pusavec, F.; Kramar, D.; Krajnik, P.; Lopac, J.: Transitioning to sustainable production-Part-II: Evaluation of sustainable machining technologies. Journal Clean Production I 18(12), 1211-1221 (2010)
6. Shokarani, A.; Dhokia, V.; Newman, S. T.: Environmentally conscious machining of difficult-to- machine materials with regard to cutting fluids. International Journal of Machine Tools Manufacturing 57, 83-101 (2012)
7. Debnath, S.; Reddy, M. M.;Yi, Q. S.: Environmental friendly cutting fluids and cooling techniques in machining: A review. Journal of Clean and Production 83, 33-47 (2014)
8. Boubekri, N.; Foster, P. R.: A technology enabler for green machining: minimum quantity lubrication (MQL). Journal of Manufacturing & management 212(5), 556-566(2015)
9. Hubner, W.; Grant, T.; Schneider, T.; Borner, H.: Tribological behaviour of materials at cryogenic temperatures. Wear 216, 150-159 (1998)

10. Ostrovskaya, Y. L.; Tukhno, T. P.; Gamulya, G. D.;Vedenlji, Y. V.; Kuleba, V. I.: Low temperature tribology at the B.Verkin Institute for Low Temperature Physics & Engineering (historical review).Tribology International 34, 265-276 (2001)
11. Yukiazu, I. Y.; Ashaboglu, F. A.; Rabinowicz, E. R.; Tachibant, T.; Kobashit, K..: Cryotribology of diamond and graphite. Cryogenics 37, 801-805 (1997)
12. Dunckle, C. G.; Aggeleton, M.; Glassman, J.; Taborek, P.: Friction of molybdenum disulfide-titanium films under cryogenic vacuum conditions,.Tribology International 44, 1819-1826 (2011)
13. Subramonian, B.; Basu, B.: Development of a high-speed cryogenic tribometer: Design concept and experimental results, Materials Science and Engineering A. 415, 72-79 (2006)
14. Hongato, L.; Hongmin, J.; Xumei, W.: Tribological properties of ultra-high molecular weight polyethylene at ultra-low temperature. Cryogenics 58,1-4 (2013)
15. Lan, P.; Gheisari, R.; Meyer, J. L.; Polycarpou, A. A., Tribological performance of aromatic thermosetting polyster (ATSP) coatings under cryogenic conditions.Wear398-399, 47-55 (2018)
16. Basu, B.; Sarkar, J.; Mishar, R.: Understanding of friction and wear mechanisms of high-purity titanium against steel in liquid nitrogen temperature, Metallurgy material Transactions. 40, 472-480 (2009)
17. Grant, T.; Schneider, T.; Borne, H.; Friction and wear at low temperature, International Journal of Hydrology Energy. 23, 397-403 (1998)
18. Theiler, G.; Grant, T.; Friction and wear of PEEK composites in vaccum environment, Wear 269, 278-284 (2010)
19. Veenstra, T. T.; Venhorst, G. C. F.; Burger, J. F.; Holland, H. J., Brake, M.; Sibri, A.; Rogalla, F.: Development of stainless steel check valve for cryogenic applications, Cryogenics 47, 121-123 (2007)
20. Wang, Q.; Zeheng, F.; Wang, T.: Tribological properties of polymers PI, PTFE and PEEK at cryogenic temperature in vacuum. Cryogenics 75, 19-25 (2016)
21. Tayeb, N. S. M. EI.; Yap, T. C.; Brevern, P. V.; Wear characteristics of titanium alloy Ti54 for cryogenic sliding applications. Tribology International 43, 2345-2354 (2010)
22. Subramoniana, B.; Kato, K.; Adachi, K.; Basu, B.: Experimental evaluation of friction and wear properties of solid lubricant coatings on SUS440C steel in liquid nitrogen, Tribology Letters 20, 263-272 (2005)
23. Basu, B.; Kumar, B. V. M.; Gilman, P. S.: Sliding wear properties of high purity copper in cryogenic environment. Journal of material Science 44, 2300-2309 (2009)
24. Mia, M.; Prithbey; Dey, R.; Hossain, M.S.; Arafat, Md. T.; Asaduzzaman, Md.; Ullah, Md. S.; Zobaer, S. M. T.: Taguchi S/N based optimization of machining parameters for surface roughness, too wear and material removal rate in hard turning under MQL cutting condition. Measurement 122, 380-391 (2018)
25. Zerti, O.; Yallease, M. A.; Khettabi, R.; Chaoui, K.; Marbrouki, T.: Design optimization for minimum technological parameters when dry turning of AISI D3 steel using Taguchi method. International Journal of Advanced Manufacturing Technology 89, 1915-1934 (2017)
26. Durakbasa, M. N.; Akdogan, A.; Vanli, A. S.; Bulutsuz, A. G.: Optimization of end milling parameters and determination of the effects of edge profile for high surface quality of AISI H13 steel by using precise and fast measurements. Measurement 68, 92-99 (2015)
27. Gunay, M.; Yucel, E.: Application of Taguchi method for determining optimum surface roughness in turning of high-alloy white cast iron. Measurement 46, 913-919 (2013)
28. Rath, D.; Panda, S.; Pal, K.: Prediction of surface quality using chip morphology with nodal temperature signatures in hard turning of AISI D3. Materials today 5, 12368-12375 (2018)
29. Aggarwal, A.;Singh, H.; Kumar, P.; Singh, M.: Optimization of multiple quality characteristics for CNC turning under cryogenic cutting environment using desirability function. Journal of

materials processing technology 205, 42-50 (2008)
30. Mandal, N.; Doloi, B.; Mondal, B., Das, R.: Optimization of flank wear using Zirconia toughned aluminia (ZTA) cutting tool: Taguchi method and Regression analysis. Measurement44, 2129-2155 (2011)
31. Nilrundra, M.; Doloi, B.; Mondal, B.: Surface roughness predication model using zirconica toughned aluminia (ZTA): Taguchi method and regression analysis. Journal of Institution of Engineers (India) Series C97 (1), 77-84 (2016)
32. Gupta, M. K.; Sood, P. K.: Optimizing multi-characteristics in machining of AISI 4340 steel using Taguchi's approach and utility concept. Journal of Institution of Engineers(India) Series C,97(1) 63-69 (2016)
33. Kumar, K. V. B. S. K.; Choudhury, S. K.; Investigation of tool wear and cutting force in cryogenic machining using design of experiments. Journal of material processing technology 203, 95-101(2008)
34. Dureja, J. S.;Singh, R.; Bhatti, M.: Optimization flank wear and surface roughness during hard turning of AISI D3 steel by Taguchi and RSM methods. Production & Manufacturing Research 2: 767-783(2014)
35. Dr. Vijay, K.; M.; Kiran , B. J., Rudresha, N.: Optimization of machining parameters in CNC turning of stainless steel (EN19) by Taguchi's orthogonal array experiments. Materials Today Proceedings 5: 11395-11407 (2018)
36. Yilmaz, B.; Karabulut, S.; Gullu, A.: Performance of analysis of new chip breaker for efficient machining of Inconel 718 and optimization of the cutting parameters. Journal of Manufacturing Processes 32, 553-563 (2018)
37. Zebia ,W.; Kowlczyk, R. Estimating the effect of cutting data on surface roughness and cutting force during WC-CO turning with PCD tool using Taguchi design and ANOVA analysis. International Journal of Advanced Manufacturing Technology 77, 2241-2256 (2015)
38. Panneerselvam,T.; Kandavel, T.K.: Kishore, P.: Experimental investigation on cutting tool performance of newly snthesized P/M Alloy Steel Under Turning Operation, Arabian Journal for Science and Engineering, (2019) https://doi.org/10.1007/s13369-019-03763-4
39. Basavarajappa, S.; Chandramohan, G.; Davim, J. P.: Application of Taguchi techniques to study dry sliding wear behaviour of metal matrix composites. Materials and Design 28, 1393-1398 (2007)
40. Kumar, S.; Nagraj, M.; Bongale, A.; Hhedkar, N.K.; Deep cryogenic treatment of AISI M2tool steel and optimization of its wear characteristics using Taguchi's approach. Arabian Journal for Science and Engineering, 1-13(2018) https;//doi.org/10.1007/s13369-018-3242-y
41. Pereira, O.; Rodriquez, A.; Abia, A. I. F.; Barreiro, J.; Lacalle, L. N. L.: Cryogenic and minimum quantity lubrication for eco-friendly turning of AISI 304. Journal of Clean Production 139, 440-449 (2016)
42. Gupta, M.K.; Sood, P.: Machining comparison of aerospace materials considering minimum quantity cutting fluid: a clean and green approach. Proceedings IMechE, Part C: Journal of Mechanical Engineering Science 231, 1445-1464 (2017)
43. Chinchnaikar, S.; Choudhary, S.K.: Machining of hardened steel- Experimental investigations, performance modelling and cooling techniques: A review. International Journal of Machine Tools & Manufacture 89, 95-109 (2015)
44. Liew, P.J.; Shaaroni, A.; Nor; Sidik, A. C.; Jiwang,Y.C.: An Overview of current status of cutting fluids and cooling techniques of turning hard steel. International Journal of Heat and Mass Transfer 114, 380-394 (2017)
45. Zerti, O.; Yallease, M. A.; Khettabi, R.; Chaoui, K.; Marbrouki, T.: Design optimization for minimum technological parameters when dry turning of AISI D3 steel using Taguchi method. International Journal of Advanced Manufacturing Technology 89, 1915-1934(2017)